

Phase correction for turbulent blurring of an image under conditions of strong intensity fluctuations

B.V. Fortes

*Institute of Atmospheric Optics,
Siberian Branch of the Russian Academy of Sciences, Tomsk*
Received February 16, 1999

Methods of adaptive optics are applied to phase correction of an optical wave propagated through a turbulent medium. It is shown by numerical simulation that requirements to an adaptive optical system (AOS) under conditions of strong intensity fluctuations remain practically the same as for weak fluctuations. Similarly, the required size of an element of a segmented mirror is equal to Fried length r_0 , and the tolerable AOS time lag is equal to r_0/V , where V is the velocity of turbulent inhomogeneities transportation. Strehl ratio in this case remains no less than 0.5. However, local slope sensors become therewith impracticable as well as the tip-tilt correction over the corrector subapertures.

1. Introduction

Propagation of optical waves through the turbulent atmosphere results first in distortion of the wave phase and then in random modulation of the intensity distribution over its cross section.¹ If the path is long enough, intensity fluctuations (IFs) become very strong. As a result, the points appear, where the intensity is zero and phase has a spiral singularity also called a wave front dislocation.² Appearance of optical wave dislocations in the turbulent medium and their influence on the operation of phase adaptive systems have been discussed theoretically in Ref. 3. Experimentally, a significant degradation of the operation efficiency of an adaptive optical system (AOS) with a flexible mirror and a Hartmann wave front sensor under conditions of strong intensity fluctuations has been observed in Ref. 4. This conclusion is in close agreement with the results of numerical simulation performed in Ref. 5.

Adaptive optical systems, which compensate for turbulent blurring of beams and images, are currently the subject of active discussions. However, it is yet to be determined how such principal AOS characteristics as the size of the corrector element needed and the tolerable time lag should be changed under conditions of strong IFs. Some problems in constructing the wave front sensor and the algorithm for phase reconstruction are also unclear as yet.

This paper considers these problems as applied to phase correction of a plane wave propagated through a randomly inhomogeneous medium with Kolmogorov spectrum of fluctuations of the refractive index. This simplified statement allows "pure" consideration of the given problem. In the general case, a number of factors affect AOS operation at adaptive correction for image blurring due to turbulence.⁶

Next, the paper considers the applicability limits of local slope sensors for the case of strong intensity fluctuations. The algorithm used allows the phase to be reconstructed from measured values of phase difference

in the presence of spiral singularities. It also allows one to minimize the reconstruction discrepancy due to measurement errors.^{12,13} The error of tip-tilt correction is analyzed. Thus, the principal restrictions on the use of the WF local slope sensors, such as Shack—Hartmann sensor and shear interferometers, are also determined.

2. Statement of the problem of numerical simulation

The problem of optical radiation propagation through a turbulent medium is stated as follows. A plane wave propagates through a homogeneous turbulent layer of the length L (Fig. 1). This layer is characterized by the intensity of turbulent fluctuations of the refractive index C_n^2 . The radiation wavelength is denoted as λ , and the wave number is $k = 2\pi/\lambda$. An AOS and a thin collecting lens are placed at the edge of the turbulent layer. The size of an AOS aperture is D . These parameters determine two characteristic scales of the problem: the cross scale, i.e., Tatarskii length of coherence ρ_0 or Fried length r_0 :

$$r_0 = (0.489 k^2 C_n^2 L)^{-3/5}, \quad \rho_0 = (1.46 k^2 C_n^2 L)^{-3/5},$$

$$r_0/\rho_0 = (1.46/0.489)^{3/5} \approx 1.93, \quad (1)$$

and the longitudinal scale, i.e. the turbulent length of diffraction $L_d = kr_0^2$. The dimensionless parameters of the problem are the scaled aperture diameter D/r_0 and the scaled path length $q = L/L_d$. The parameter q is related to the scintillation index β_0^2 , which corresponds to the relative variance of plane wave intensity fluctuations in Rytov approximation¹:

$$\beta_0^2 = 1.24 C_n^2 k^7 L^{11/6} = \frac{1.24 \left(\frac{L}{kr_0^2} \right)^{5/6}}{1.46 \left(\frac{L}{kr_0^2} \right)^{5/6}} =$$

$$= \frac{1.24}{0.489} \left(\frac{L}{kr_0^2} \right)^{5/6} = 2.54 q^{5/6}. \quad (2)$$

Note that the turbulent length of diffraction is determined through Fried length r_0 rather than Tatarskii length ρ_0 . Equations (1) and (2) give the relation between them.

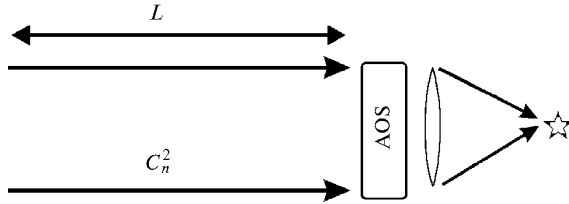


Fig. 1. Wave propagation geometry.

The propagation of a plane wave is described by the parabolic equation

$$2ik \frac{\partial U}{\partial z} = \left(\frac{\partial^2}{\partial x^2} + \frac{\partial^2}{\partial y^2} + 2k^2(n-1) \right) U \quad (3)$$

for the complex amplitude U . The amplitude U is related to the scalar field strength E by the equation $E(x, y, z) = U(x, y, z) \exp \{ ikz - i\omega t \}$. Here $n-1 \ll 1$ are the random fluctuations of the refractive index $n(x, y, z)$; ω is the frequency of the electromagnetic oscillations. The equation is supplemented with the boundary conditions for the plane wave that is being propagated along the axis OZ :

$$U(x, y, z = 0) = 1. \quad (4)$$

It can be solved numerically using the splitting method^{7,8} following a symmetrized scheme. Random phase screens were simulated by the technique described in Refs. 9 and 10. The complex amplitude and phase screens were simulated on a uniform 128×128 computational grid. The aperture of the collecting lens was placed at the central part of the grid with the size 64×64 pixels. So, at $D/r_0 = 10$ the grid step was 6.4 times less than the coherence length. The random medium was stimulated by six phase screens. Instant distributions of the intensity at the lens focus were averaged over 50 independent random realizations.

3. Adaptive system with a constant time lag

Consider the influence of a time lag on the operation efficiency of the AOS with an ideal sensor and a phase corrector. The phase correction φ in this case is determined through the argument of the complex amplitude:

$$\varphi(\rho, t) = \arg (U(\rho, t - \tau)), \quad \rho = (x, y), \quad (5)$$

where U is the complex amplitude of the field, as it leaves the turbulent medium, in the plane $z = L$; τ is the time lag introduced by the AOS; t is time; \arg

denotes the principal value of the argument of a complex parameter.

In the case of weak intensity fluctuations, at $\tau V \ll D$, the variance of the residual phase distortions is equal to the structure function, D_φ , of the phase :

$$\sigma^2 \approx D_\varphi(\tau V) = 6.88 (\tau V / r_0)^{5/3}. \quad (6)$$

The scaled intensity at the lens focus (Strehl parameter) can be approximately estimated as

$$SR \approx \exp (-\sigma^2) = \exp [-6.88 (\tau V / r_0)^{5/3}]. \quad (7)$$

A decrease in the Strehl parameter characterizes degrading efficiency of the AOS. The latter is apparently dependent on how the phase φ changes during the time τ . In the approximation of frozen turbulence (Taylor hypothesis) and provided that the wind vector V is independent of the longitudinal coordinate z , the change in the phase occurring during the time τ corresponds to the phase difference at the points separated by the distance $\Delta\rho = \tau V$.

In the vicinity of wave front dislocations, the phase changes very rapidly. Therefore, it would be expected that in the region of strong IFs the dependence of the AOS operation efficiency on the time lag τ becomes stronger. However, results of numerical simulation show that it is not the case. Figure 2 shows three versions of the dependence $SR(\tau V / r_0)$. One of them corresponds to calculation by Eq. (7); two others, which are the results of numerical simulation for weak fluctuations ($q = 0.1$) and strong fluctuations ($q = 1$), practically coincide. The difference between the results of numerical simulation and calculation by Eq. (7) can be explained by two reasons. The one may be the overestimation of the variance of residual distortions when calculated by Eq. (6) and the other one may be in the absence of inhomogeneities with the scales larger than the size of the computational grid (equal to $2D$) in the simulated phase screens.

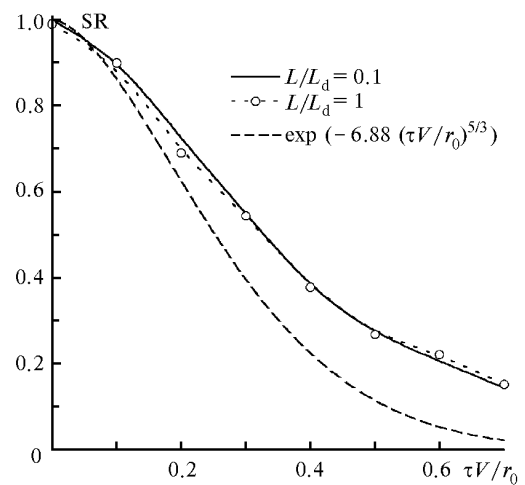


Fig. 2. Strehl parameter, SR, as a function of the scaled time lag in the AOS with a constant lag.

Thus, the operation efficiency of AOS with a constant time lag insignificantly depends on the variance of the intensity fluctuations. This is likely explained by the fact that regions with fast changes in the phase (these regions are adjacent to wave front dislocations) are small and do not contribute significantly to the radiation power collected in the focal spot.

4. Adaptive system with a segmented mirror

Flexible adaptive mirrors with a continuous surface are ill-suited to correction under conditions of broken continuity of the wave front. Therefore, segmented mirrors are more promising for operation under conditions of strong fluctuations. Positions of individual elements in such correctors are independent, and the surface formed by them can be discontinuous. Discontinuity of the wave front can certainly be approximated by the surface of a flexible mirror as well, but this requires a far larger number of control elements.

To construct an AOS with the given level of operation efficiency, one needs to know the corresponding size of an element of a segmented mirror. In the region of weak intensity fluctuations, we can use the following equation for the variance of residual phase distortions σ^2 :

$$\sigma^2 = 1.03 (d/r_0)^{5/3}. \tag{8}$$

This equation corresponds to the variance of phase fluctuations within a circle of diameter d after subtraction of the average phase.¹¹ In correcting for the average phase and the local tilts at every element of the segmented mirror, the variance of residual phase distortions is

$$\sigma^2 = 0.134 (d/r_0)^{5/3}. \tag{9}$$

The estimate of Strehl parameter as $SR = \exp(-\sigma^2)$ at $d = r_0$ gives the following values: $SR = 0.36$ when correcting for the average phase and $SR = 0.87$ when correcting for both the average phase and local tilts.

If dislocations arise, unambiguous determination of the phase at the aperture becomes impossible. It also becomes impractical to control tip and tilt of an element by averaging the phase and its gradient over the aperture. Therefore, to study the influence of the size of the corrector element on the efficiency of the adaptive system operation in the case of strong fluctuations, define the phase correction on the area of size d in the following way:

$$\varphi + k \mathbf{S} \mathbf{\rho}, \tag{10}$$

where φ , S_x , and S_y are corrections of the average phase and the local tilts, respectively. These parameters can be determined from the complex amplitude averaged over a subaperture

$$\varphi = \arg(\bar{U}); \quad \bar{U} = \frac{1}{d^2} \int d^2 \rho U(\rho) \tag{11}$$

and the weighted mean phase gradient

$$\mathbf{S} = \frac{1}{kP} \int d^2 \rho I(\rho) \nabla \varphi(\rho) = \frac{1}{kP} \int (\text{Re } U \nabla \text{Im } U - \text{Im } U \nabla \text{Re } U) d^2 \rho. \tag{12}$$

Here the integral is taken over the area corresponding to the corrector element (subaperture) of the size d ; $I(x, y) = U U^*$ is the incident radiation intensity; k is the wave number; P is the power at the subaperture,

$$P = \int d^2 \rho I(\rho). \tag{13}$$

This equations allow us to determine control over the corrector, while avoiding determination of the wave phase. They use the complex amplitude U known from numerical simulation as the initial parameter.

Figure 3 shows the dependence of the SR parameter on the scaled path length $q = L/L_d$. Note quite good agreement between the results obtained and the above estimates by Eqs. (8)–(9) for the case of weak intensity fluctuations. The results presented indicate that the efficiency of this correction slightly depends on the scaled path length, which characterizes the level of intensity fluctuations. Moreover, practically no such dependence is observed in the case of correction only for the average phase (without correction for local tilts). On the contrary, even a slight growth of the SR parameter in the region $0 < L/L_d < 0.4$ is observed. This can be explained by the diffraction-induced transformation of the small-scale part of phase fluctuations into the amplitude ones and the corresponding decrease in the residual phase distortions.

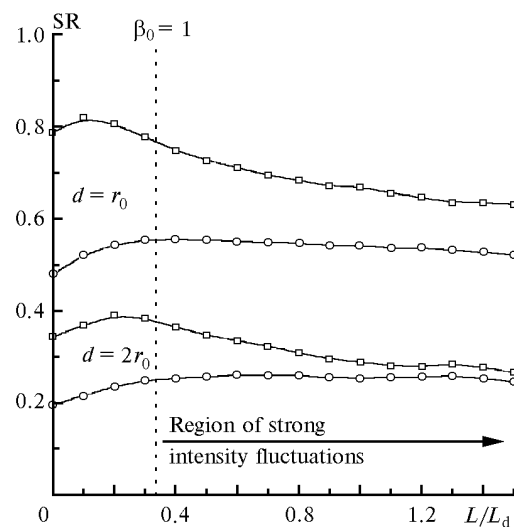


Fig. 3. Strehl parameter, SR, as a function of the normalized path length $L/(kr_0^2)$ in the adaptive system with a segmented mirror: control over tips of corrector elements (circles), control of tips and tilts (squares).

Note that when both the average phase and local tilts are corrected, the AOS efficiency decreases a little bit. However, it remains higher than the efficiency of an AOS with the correction of only the average phase. For $d = 2r_0$ the difference between these two versions of AOS becomes smaller than 10% at $L/L_d > 1$.

Thus, the AOS with a segmented mirror, the size of whose elements is less than or equal to the coherence length r_0 , can ensure high quality of correction both for the case of weak and strong intensity fluctuations. The corresponding value of Strehl parameter is no less than 0.5–0.8 depending on the IF level and the number of degrees of freedom of each element. The restrictions on the time lag introduced by an AOS do not become stricter. Therefore, the main problem is to construct the corresponding wave front sensor.

5. Algorithm for reconstruction of the phase matrix

Consider first the problem of phase reconstruction from known values of the phase difference (PhD) between the subapertures. The sought value here is the phase assigned to every subaperture as a whole, for example, the phase of the mean complex amplitude (11).

The problem of reconstructing the phase matrix has been intensively discussed in the literature.^{14–17} In the majority of papers dealing with this problem, algorithms minimizing the influence of measurement errors by the method of least squares have been considered with a slightly varying problem geometry. In those considerations, it has been proposed that with no errors the sum of initial PhDs over any closed path is zero.

This assumption is clearly invalid in the presence of spiral dislocations of the phase. If the point of dislocation is inside a closed path, then the sum of PhDs is equal to 2π and the standard method of least squares gives wrong solution even in the absence of measurement errors in the PhD. Therefore, application of the corresponding algorithms of phase reconstruction is restricted to the region of weak IFs.

This restriction has been removed in Ref. 12, where it was proposed to modify the initial array of PhDs by adding $2\pi \times (\text{integer number})$ to elements of this array so that the absolute value of the PhD sum over any minimal path equals zero with no measurement errors and does not exceed π in the presence of some errors. If the problem is formulated on a uniform square grid with the size $N \times N$, then implementation of the corresponding algorithm of phase reconstruction with the use of the discrete Fourier transform creates no problems.¹³ According to Refs. 12 and 13, we refer to the usual formulation of the problem of phase reconstruction by the method of least squares (unmodified) as a normal equation (NE), while the modification proposed in Refs. 12 and 13 is referred to as a modified normal equation (MNE).

We have implemented the algorithms for solution of NE and MNE in such a way that the sought phase matrix $\varphi_{i,j}$, $i, j = 1, 2, \dots, N$ was calculated from two arrays of estimates $\Delta_{i,j}^x$ and $\Delta_{i,j}^y$, each having the size $N \times (N - 1)$. To check the algorithm and the program implementing it, true PhD values found in the numerical experiment from the known complex amplitude were substituted to the arrays $\Delta_{i,j}^x$ and $\Delta_{i,j}^y$. This substitution gave just the same value of the SR parameter as the above-considered simulation of the AOS with a segmented mirror.

6. Measurement of the phase difference

Today's wave front sensors capable of operating in real time under conditions of atmospheric turbulence are the sensors of local tilt. Among them there are modifications of Hartmann sensor and shear interferometers. In both cases, the output signal from every element of a sensor is proportional to the weighted mean gradient of the phase at its subaperture, and the weight is equal to the intensity of incident optical wave:

$$\mathbf{g} = \frac{1}{P} \int d^2 \rho I(\rho) \nabla \varphi(\rho) \quad (14)$$

(in the shear interferometer, the instrumental weight function is added¹⁸). The phase difference between the subaperture edges is calculated as a product of the output signal by the subaperture size:

$$\Delta^x = g_x d, \quad \Delta^y = g_y d. \quad (15)$$

If a corrector with the same configuration and same size of elements is used in combination with Hartmann sensor, then measurement errors in the phase differences can be decreased by using two Hartmann sensors – one for each of the PhD arrays $\Delta_{i,j}^x$ and $\Delta_{i,j}^y$. In our numerical experiments, the results of which are presented below, three sensors of the local tilts were used:

- sensor I (to measure $\Delta_{i,j}^x$) of $(N - 1)N$ size, shifted along the coordinate x by $d/2$ relative to the corrector elements;

- sensor II (to measure $\Delta_{i,j}^y$) of $N(N - 1)$ size, shifted along the coordinate y by $d/2$ relative to the corrector elements;

- sensor III (unshifted, of $N \times N$ size) to control tilts of the corrector elements.

The values of $\varphi_{i,j}$ calculated from PhD arrays of the first two sensors are used to control shifts of the corrector elements, while the values of $g_{i,j}$ from the third sensor are used to control tilts of the elements. Maybe such a configuration is not optimal, but in the limiting capabilities it is very close to optimum.

7. Results of simulation of an AOS with a sensor of local tilts

The above-described scheme of the AOS with three sensors of local tilts has been used in numerical experiments on the efficiency of compensation for turbulent blurring of an image. Local tilts were calculated by the following equations:

$$g_x = \frac{1}{P} \int \left(\text{Re } U \frac{\partial \text{Im } U}{\partial x} - \text{Im } U \frac{\partial \text{Re } U}{\partial x} \right) d^2 \rho,$$

$$g_y = \frac{1}{P} \int \left(\text{Re } U \frac{\partial \text{Im } U}{\partial y} - \text{Im } U \frac{\partial \text{Re } U}{\partial y} \right) d^2 \rho,$$

where the integral is taken over a subaperture with the size d . The derivatives with respect to x and y were found by multiplying the discrete Fourier transforms of the real and imaginary parts of the complex amplitude by the corresponding filtering function.

The phase correction at the i, j th corrector element was set in the following way:

$$\varphi_{i,j} + g_x x + g_y y, \tag{16}$$

where g_x and g_y are local tilts measured with sensor III, and φ_{ij} is the phase matrix obtained by solving MNE with the PhD arrays from sensors I and II.

All calculations have been performed for $D/r_0 = 10$ and for $D/d = 10$. Thus, the size of the subaperture of a sensor and corrector was equal to Fried length r_0 .

Figure 4 shows the dependence of Strehl parameter on the scaled path length L/kr_0^2 for the following versions of the numerical experiment: solution of NE at $d \rightarrow 0$ (curve 1); solution of NE at $d = r_0$ (curve 2); solution of MNE at $d = r_0$ (curve 3).

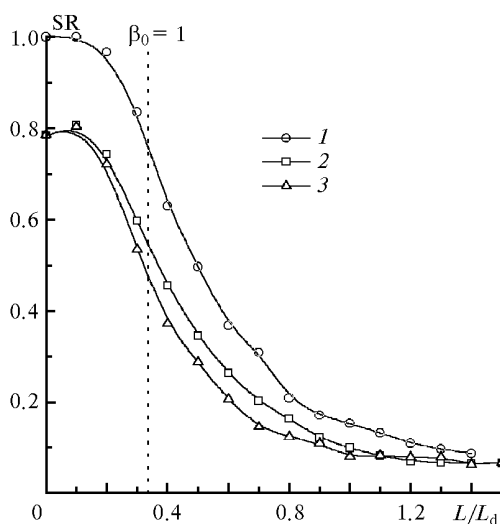


Fig. 4. The SR parameter as a function of the scaled path length L/kr_0^2 for different versions of the sensor.

In the considered numerical experiment, the condition $d \rightarrow 0$ means that the size of the element is equal to the distance between nodes of the computational grid, and the phase differences are determined directly from the values of the complex amplitude without calculation of the local tilts.

The presented dependence $SR(L/L_d)$ indicates that the efficiency of correction rapidly degrades in the region of strong fluctuations ($\beta_0 > 1$) when using NE. It also turned out that the AOS operation efficiency degrades even somewhat faster when using MNE. The decrease of the size of an element d also does not result in an increase of the SR parameter. Therefore, we should accept that an AOS with the sensor of local tilts is impracticable under conditions of strong IFs even with the use of the algorithm for phase reconstruction (the algorithm has been specially constructed for reconstructing the phase matrix in the presence of spiral dislocations).

To reveal the cause of this failure, we have studied the dependence of the variance of error in estimation of the phase difference on the normalized path length. The error for the i, j th subaperture of the sensor was calculated in the following way:

$$\varepsilon_{i,j} = \left(\arg \overline{U}_{i+1,j} - \arg \overline{U}_{i,j}^* \right) - g_x i,j \cdot d, \tag{17}$$

where the overbar denotes averaging over the subaperture of sensor III. This subaperture coincides with the area of the corrector element. In Eq. (17) g_x is the weighted-mean gradient of the phase at the corresponding subaperture of sensor I. The value of the error ε_{ij} was reduced to the range $(-\pi, \pi]$. The variance of the error was estimated by averaging over all subapertures and 10 random realizations.

Figure 5 illustrates the growing variance of tip-tilt correction error with the increasing ratio L/L_d , which characterizes the IF variance. It is seen that the variance of the error increases rather fast, what is the explanation of the decrease in the efficiency of the AOS with a sensor of local tilts.

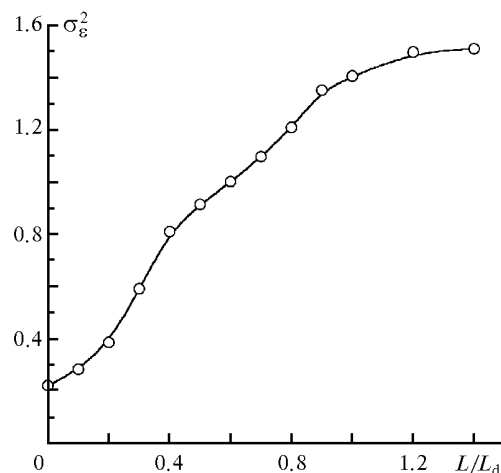


Fig. 5. The variance of tip-tilt correction error vs. the scaled path length.

To achieve a gain from the use of MNE, one needs to have a sensor capable of measuring the phase difference more accurately under conditions of strong intensity fluctuations. In principle, the phase difference can be estimated from the position of the interference fringe resulting from interaction of fields coming from neighboring subapertures of an AOS. However, it may prove rather hard to perform such measurements in real time under conditions of atmospheric turbulence.

Let us make some remarks about the scaled aperture diameter D/r_0 . The results presented have been obtained at a fixed value $D/r_0 = 10$. Preliminary calculations for $D/r_0 > 10$ have shown that as the AOS efficiency decreases, the SR parameter decreases somewhat faster and tends to its value in the system without an adaptive correction. The larger the scaled diameter D/r_0 , the smaller the latter value.

8. Conclusions

Thus, the efficiency of phase compensation for turbulent blurring of an image has been studied for the case of strong IFs. The calculations have shown that the critical point of an AOS construction is the sensor of wave front distortions. The use of a segmented mirror gives practically the same values of Strehl parameter ($SR \cong 0.5$ at $d = r_0$) for both weak and strong IFs, when correcting only the average phase. When correcting both the average phase and the local tilts, the efficiency of AOS operation becomes somewhat lower in the region of strong IFs. However, it remains higher than for an AOS with correction of only the average phase. Both versions of the AOS have nearly the same efficiency at long path lengths L/L_d . Therefore, when designing an AOS for operation under conditions of strong IFs, correction of local tilts can be rejected. Thus, the AOS design becomes much simpler.

The situation with the sensor of wave front distortions is just similar. Measurements of local tilts become impractical under conditions of strong intensity fluctuations, because the correlation between the local tilt and the phase difference becomes weaker with increasing IFs. To extend the AOS application to the region of strong IFs, the sensor should be constructed following the principle of direct measurement of the phase difference. Besides, the modified normal equation should be used for solution of the problem on phase reconstruction.

Dynamic characteristics of an AOS have been considered using, as an example, the correction with a constant time lag, all other factors being neglected. The calculations have shown that influence of a constant time lag on the AOS efficiency is independent of the level of IFs. The combination of time lag correction with other factors can possibly give a more complex pattern.

Spectral characteristics of the adaptive correction remained beyond the scope of this paper. Under conditions of strong intensity fluctuations, the AOS is most likely very sensitive to the difference between wavelengths of a reference beam and the beam to be corrected, because scaling of phase correction from one wavelength to another under conditions of broken phase continuity is rather problematic.

References

1. V.I. Tatarskii, *Wave Propagation in a Turbulent Medium* (Dover, New York, 1968).
2. N.B. Baranova and B.Ya. Zel'dovich, *Zh. Eksp. Tekh. Fiz.* **80**, 1789 (1981).
3. D.L. Fried and J.L. Vaughn, *Appl. Opt.* **31**, No. 15, 2865–2882 (1992).
4. C.A. Primmerman, T.R. Price, R.A. Humphreys, B.G. Zollars, H.T. Barclay, and J. Herrmann, *Appl. Opt.* **34**, No. 12, 2081–2089 (1995).
5. V.P. Lukin and B.V. Fortes, in: *Abstracts of Reports at the Third International Symposium on Atmospheric and Oceanic Optics*, Tomsk (1996), pp. 28–29.
6. V.P. Lukin, *Atmospheric Adaptive Optics* (Nauka, Novosibirsk, 1986), 286 pp.
7. J.A. Fleck, J.R. Morris, and M.D. Feit, *Appl. Phys.* **10**, No. 1, 129–139 (1976).
8. P.A. Konyaev, in: *Abstracts of Reports at VII All-Union Symposium on Propagation of Laser Radiation through the Atmosphere* (Tomsk Scientific Center of the Siberian Branch of the USSR Academy of Sciences, Tomsk, 1983), pp. 104–106.
9. V.P. Lukin, N.N. Maier, and B.V. Fortes, *Atm. Opt.* **4**, No. 12, 896–899 (1991).
10. B.V. Fortes and V.P. Lukin, *Proc. SPIE* **1668**, 477–488 (1992).
11. R.J. Noll, *J. Opt. Soc. Am.* **66**, No. 3, 207–211 (1976).
12. H. Takajo and T. Takahashi, *J. Opt. Soc. Am. A* **5**, No. 3, 416–425 (1988).
13. H. Takajo and T. Takahashi, *J. Opt. Soc. Am. A* **5**, No. 11, 1818–1827 (1988).
14. D.L. Fried, *J. Opt. Soc. Am.* **67**, No. 3, 370–375 (1977).
15. R.H. Hudgin, *J. Opt. Soc. Am.* **67**, 375–378 (1977).
16. B.R. Hunt, *J. Opt. Soc. Am.* **69**, 393–399 (1979).
17. J. Herrmann, *J. Opt. Soc. Am.* **70**, 28–35 (1980).
18. L. Goad, F. Roddier, J. Becker, and P. Eisenhardt, *Proc. SPIE* **628**, 305–313 (1986).